Ann. Geophysicae 16, 821–827 (1998) © EGS – Springer-Verlag 1998

Annales Geophysicae

Incoherent scatter radar observations of AGW/TID events generated by the moving solar terminator

V. G. Galushko[1], **V. V. Paznukhov**[1], **Y. M. Yampolski**[1], **and J. C. Foster**[2]

[1] Institute of Radio Astronomy, National Academy of Sciences of Ukraine, Kharkov, Ukraine
[2] MIT Haystack Observatory, Atmospheric Sciences Group, Westford, MA 01886, USA

Received: 13 October 1997 / Revised: 6 February 1998 / Accepted: 10 February 1998.

Abstract. Observations of traveling ionospheric disturbances (TIDs) associated with atmospheric gravity waves (AGWs) generated by the moving solar terminator have been made with the Millstone Hill incoherent scatter radar. Three experiments near 1995 fall equinox measured the AGW/TID velocity and direction of motion. Spectral and cross-correlation analysis of the ionospheric density observations indicates that ST-generated AGWs/TIDs were observed during each experiment, with the more-pronounced effect occurring at sunrise. The strongest oscillations in the ionospheric parameters have periods of 1.5 to 2 hours. The group and phase velocities have been determined and show that the disturbances propagate in the horizontal plane perpendicular to the terminator with the group velocity of 300–400 m s^{-1} that corresponds to the ST speed at ionospheric heights. The high horizontal group velocity seems to contradict the accepted theory of AGW/TID propagation and indicates a need for additional investigation.

Key words. Ionosphere (wave propagation) · Meteorology and atmospheric dynamics (waves and tides)

1 Introduction

Investigations of the atmospheric gravity waves (AGW) manifesting themselves at ionospheric heights as traveling ionospheric disturbances (TID) are of great importance due to their role in the energy and momentum exchange between different regions of the upper atmosphere. A distinctive characteristic of this kind of wavelike disturbances is their persistence (the main AGW parameters such as spatial periodicity, velocity and direction of motion are retained over great distances from their origin). Hines (1960) was the first to give a fundamental explanation of AGWs and their relationship to TIDs. Since then, a number of review papers (Yeh and Liu, 1972; Hines, 1974; Francis, 1975; Hines, 1980; Hunsucker, 1982; Mayr *et al.*, 1990; Crowley, 1991; Leitinger, 1992; Hocke and Schlegel, 1996) have described the essential results of AGW/TID research. Gravity waves in the upper atmosphere can be observed either directly as neutral gas fluctuations (for example, with the use of interferometers or satellite-borne mass spectrometers) or indirectly as ionospheric plasma variations using various remote radio techniques (incoherent scatter, IS, HF Doppler, TEC, etc.). But despite the extensive research that has been performed, there are still many open questions in the problem of the generation and propagation of AGWs/TIDs.

AGWs can be generated by different sources either of natural or anthropogenic origin (particle precipitation at high latitudes, moving solar terminator, jet streams, wind shears, earthquakes, hurricanes, tsunami or industrial accidents, ionosphere modification experiments, powerful blasts, chemical releases, etc.). It is worth noting that among all the sources of gravity waves, the moving solar terminator (ST) has a special status since it is a predictable phenomenon whose characteristics are well known. The ST is characterized by sharp changes in atmospheric parameters such as energy, temperature, pressure, and electron density at a given altitude. The main energy source, the solar heat input and its absorption, depends on the photochemistry of the atmosphere together with convection and diffusion effects. In the vicinity of the ST, the atmospheric gas is not in an equilibrium state. This situation and the motion of the ST cause both waves and turbulence. Such processes have been reviewed by Somsikov and Ganguly (1995). Considering the ST as a stable and repetitive source of AGWs, one can derive information

Correspondence to: J. C. Foster

about atmospheric conditions from the response of the medium to this input. Such a source is suitable for investigating gravity wave parameters and could be used as an atmospheric diagnostic, using the ST-generated waves as probe signals. However, experimental measurements of the effects of the solar terminator as a generation region for AGWs are quite rare (Bezrodny *et al.*, 1976; Popov and Yampolsky, 1981; Galushko and Yampolski, 1983; Beley *et al.*, 1995). The work reported here was directed towards determining the main parameters of ST-generated AGWs/TIDs through a set of specifically designed and analyzed incoherent scatter radar observations.

2 Experiments

Experimental observations were obtained with the high-powered UHF (440 MHz) incoherent scatter radar at the Millstone Hill Observatory (42.6°N, 288.5°E). Ionospheric data investigated include electron density, electron temperature, ion temperature, and ion drift velocity observed along the line of sight of the fully steerable 46-meter or the zenith-directed 68-m antenna. An initial investigation sought direct evidence in the radar data of an ionospheric response to the passage of the solar terminator used previously-acquired data from a March 1992 zenith-directed, fixed-beam, radar experiment. Spectral analysis identified low-frequency disturbances with the period of more than 1 h which were generated by the ST. Subsequently, special experiments were carried out during the autumn of 1995 to investigate further these wavelike disturbances, and to determine their main parameters such as spatial periodicity, velocity, and direction of motion. These dedicated experiments were performed in near-equinox conditions when the terminator is best aligned along the meridian and were designed to look for the altitude/latitude signatures, predicted by the ST/AGW-generation theory. To investigate altitude and space/time effects, a three-beam operating mode was chosen, whose scheme is shown in Fig. 1. Switching between antenna positions in the sequence "zenith-west-zenith-north-zenith" was done with a cycle time of 5 min and data were integrated in each position for 68 s. Hence, the sampling time was equal to 5 min for positions "west" and "north" and 2.5 min for the zenith position. Ionospheric parameters were determined over the height range 154 km–427 km with a height resolution of ~20 km.

In order to determine TID characteristics unambiguously, we need to have $\Delta t < T/2$, where Δt is the data sampling time and T is the period of the TID. Spatial sampling is done with ΔL^h_{Z-W}, $\Delta L^h_{Z-N} < \Lambda$, where ΔL^h_{Z-W}, ΔL^h_{Z-N} are the horizontal spatial distances between positions "zenith-west" and "zenith-north" at height, h, and Λ is the TID wavelength. As follows from theoretical works (e.g. Somsikov, 1983; Somsikov and Ganguly, 1995) the temporal period and spatial scale of ST-generated TIDs depend on the Mach number $M = V_T/V_S$, where V_T is the velocity of the ST and V_S is the sound velocity. At mid-latitudes, three regions of the atmosphere can be differentiated based on the magnitude of M. The first corresponds to inequality $M^2 > 1$ and is located below the altitude of 120 km. Both acoustic and gravity waves can be generated in this region. The second region lies between 120 km and 180 km where $1 > M^2 > 0.8$. The waves generated by the ST in this region, as a rule, are decaying. Finally, a third region where $M^2 < 0.8$ begins from ~180 km and stretches up to 600 km. In this region the ST generates gravity waves with a spatial scale of about 1000 km and with period more than 30 min. Taking into account the location of the Millstone Hill Observatory and the height range where the measurements of the ionospheric parameters were performed, one concludes that these experiments are most likely to observe TIDs related with gravity waves with spatial scales of a few hundreds of kilometers.

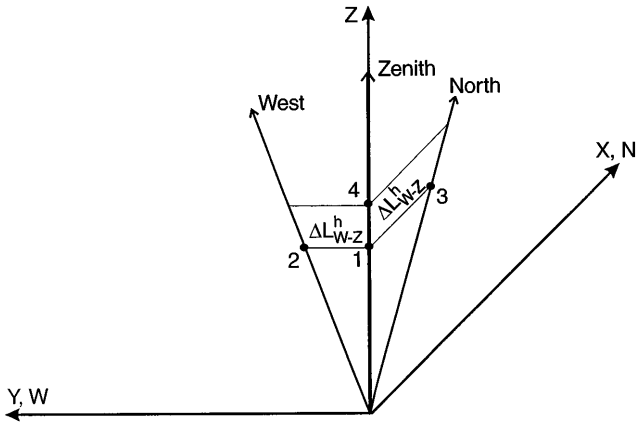

Fig. 1. Schematic representation of the 3-beam radar experiment used to determine TID/AGW propagation characteristics. Radar beams at 40° elevation angle to the north and the west were interleaved with vertical observations with the Millstone Hill zenith antenna

It is known (Hargreaves, 1982) that gravity waves have frequencies less than Brunt-Väisälä frequency, ω_B. For the height range where the measurements were carried out, the period corresponding to ω_B is $T_B = 1/\omega_B \approx 10\,\text{min}$. Therefore, the shortest expected TID period is equal to 10 min and an experimental sampling time of 5 min was chosen. For a rough estimate of TID wavelength, we assume that the disturbances move at the velocity of the ST, which varies slightly over the height range of interest. For 240 km (near the height of the daytime electron density maximum), the TID period was assumed to be equal to the shortest period expected, 10 min. Thus, the shortest expected wavelength is $\Lambda = V_T \times T = 360\,\text{km s}^{-1} \times 600\,\text{s} = 216\,\text{km}$.

So, it is necessary that ΔL^{240}_{Z-W} and ΔL^{240}_{Z-N} be less than 216 km. In our measurements they both were chosen to equal 200 km by setting the elevation angle of antenna beams to be 40° from vertical. As mentioned already, the most likely TID periods are expected to be greater than 30 min, and therefore the experiment plan was well matched to its objectives.

3 Data processing

Of the four ionospheric parameters investigated, the ST-generated disturbances were most consistently observed in the electron density data. Segments of electron density records obtained on September 21, 1995 are shown in Fig. 2. Curves for different heights are artificially shifted to avoid overlapping. Times of the sunset and sunrise terminator passage at ionospheric heights over the observatory are indicated. The ST-generated disturbances manifest themselves as a "peak" in electron density at sunset as well as "fast" oscillations after sunrise. However, the pronounced diurnal trend of the parameters makes it difficult to observe the effect of AGWs/TIDs generated by the ST and complicates their spectral analysis. Accordingly, the data were detrended before further processing by subtracting data smoothed by a moving rectangular time window. Disturbances with periods >2.5 h–3 h can be associated with tidal modes (Hocke, 1996), so a smoothing window width of 2.5 h was chosen to remove variations which were not associated with the ST. This slowly varying trend, $\langle N \rangle$, was subtracted from the original density data to yield the time-varying part of the electron density record, $\delta N = N - \langle N \rangle$, which was further analyzed with a stepped Fourier transform

$$S(\omega, T_s + n \cdot \Delta t) = \int_{T_s + n \cdot \Delta t}^{T_s + n \cdot \Delta t + T_j} \mathrm{d}t \delta N e^{-j\omega t} \qquad (1)$$

which determines a time-sequence of spectra where Δt is the step between adjacent spectra, $n = 1, 2, 3, \ldots,$ T_j is the integration time, $\omega = 2\pi f$ is the angular frequency, T_s corresponds to the start of the records. The results of applying this procedure to the data collected in the zenith position on September 21, 1995 are presented in Fig. 3 where T_j was 2.5 h, and Δt was 10 min (2 samples). Some strengthening of the spectral intensity after sunrise and sunset over a wide height range is apparent. It is worth noting that the strengthening of the fluctuations does not occur across the entire frequency range, but only at selected frequencies (this is quite evident for the spectra at 301 km). Such spectral fine structure indicates the presence of wavelike processes in the ionosphere. From Fig. 3 one can see that the most powerful spectral components are concentrated within the frequency band which corresponds to time periods of 1.5–2.5 h. The most powerful spectral components then were selected by a numerical rectangular filter. The band-pass filter had cutoff frequencies corresponding to the time periods $T_{min} = 90$ min and $T_{\max} = 130$ min. Figure 4 demonstrates filtered data for the three antenna positions ("zenith", "west", and "north"). The spatial/temporal structure of the disturbance is represented by the isolines of electron density and the intensity of the fluctuations is given in gray scale. The maximum intensity of the disturbances is observed near the solar terminator. It is clearly seen that the effect is not over the whole height range, but occurs only at heights lower than ~300 km.

We have used a triangular method to determine TID characteristics, including velocity and direction of motion. To estimate these parameters, measurements are needed in four different points, not in the same plane (Fig. 1, points 1–4). To determine time delays between variations for different measuring points, cross-correlation analysis was applied to the filtered records near the time of ST passage for positions "zenith", "west", and "north" and results are given in Table 1. The cross-correlation values are sufficiently high over the height range 217–301 km to conclude that the disturbances are moving as "frozen-in irregularities", i.e., all spectral components move with the same velocity. The time delays between variations for the different points were derived from the maxima of the correlation functions. TID group velocity, V_g, and direction of motion were

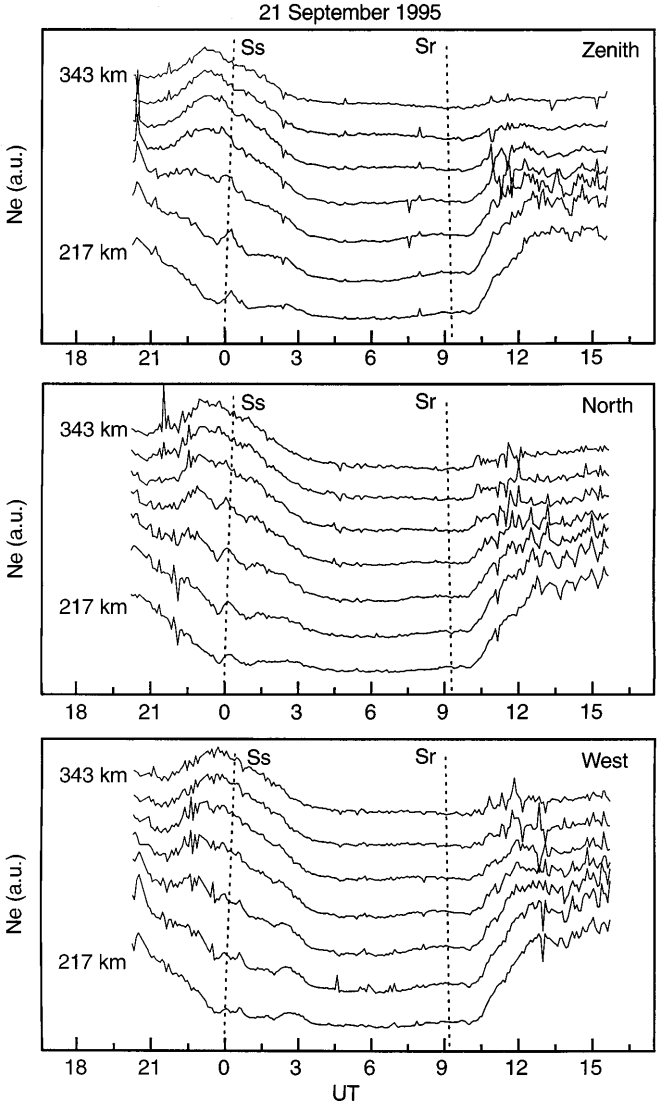

Fig. 2. Unfiltered electron density observations (log 10) observed at several altitudes during the dedicated TID experiment on September 21, 1995 are shown for the three antenna positions of Fig. 1. *Curves* for different heights are artificially shifted to avoid overlapping. Times of the sunset and sunrise terminator passage at ionospheric heights over the observatory are indicated

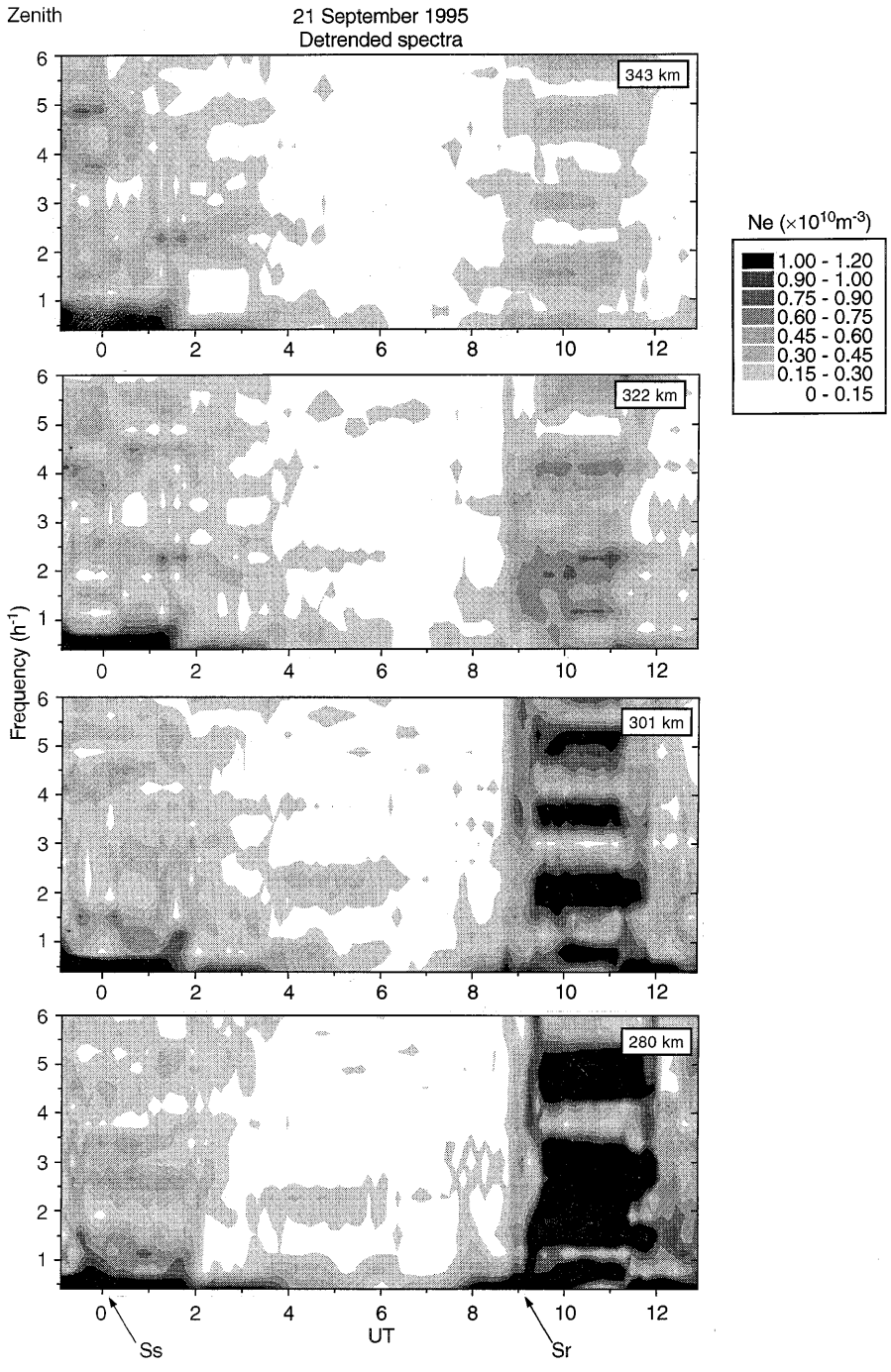

Fig. 3. Spectral power of the detrended density data at four *F*-region altitudes reveal strong intensification of wavelike (banded) disturbances in the two hours following sunrise (at ~09 UT). The most powerful spectral components correspond to temporal periods of 1.5 h–2.5 h

determined for the height range where values of cross-correlation functions were high. The results of these estimates of V_g are given in Table 2. In the frame of reference where V_g was derived, γ is elevation angle and ϕ is azimuth measured counter-clockwise from the north. TID phase velocity was determined as the velocity of a monochromatic wave. To estimate the phase velocity of the TID motion, the strongest spectral component (2*h*-wave) was selected from the spectrum of the filtered records. Phase differences between variations for four measuring points were derived from the cross-spectra. Propagation velocity of the 2*h*-wave was estimated as the speed of motion of a plane wave. The phase velocity and direction of propagation of the strongest component of the wave packet are given in Table 3.

We are able to determine the spatial wavelength of the disturbances from the temporal period and velocity of the TIDs motion. Figure 5 illustrates V_{ph} versus Λ dependencies which follow the dispersion law for ionospheric wavelike processes. The data were derived for the most powerful spectral harmonics of the electron density variations for different heights. It is evident that for longer wavelengths, the wave moves faster. A similar behavior of AGWs has been mentioned by other authors (e.g. Hocke and Schlegel, 1996).

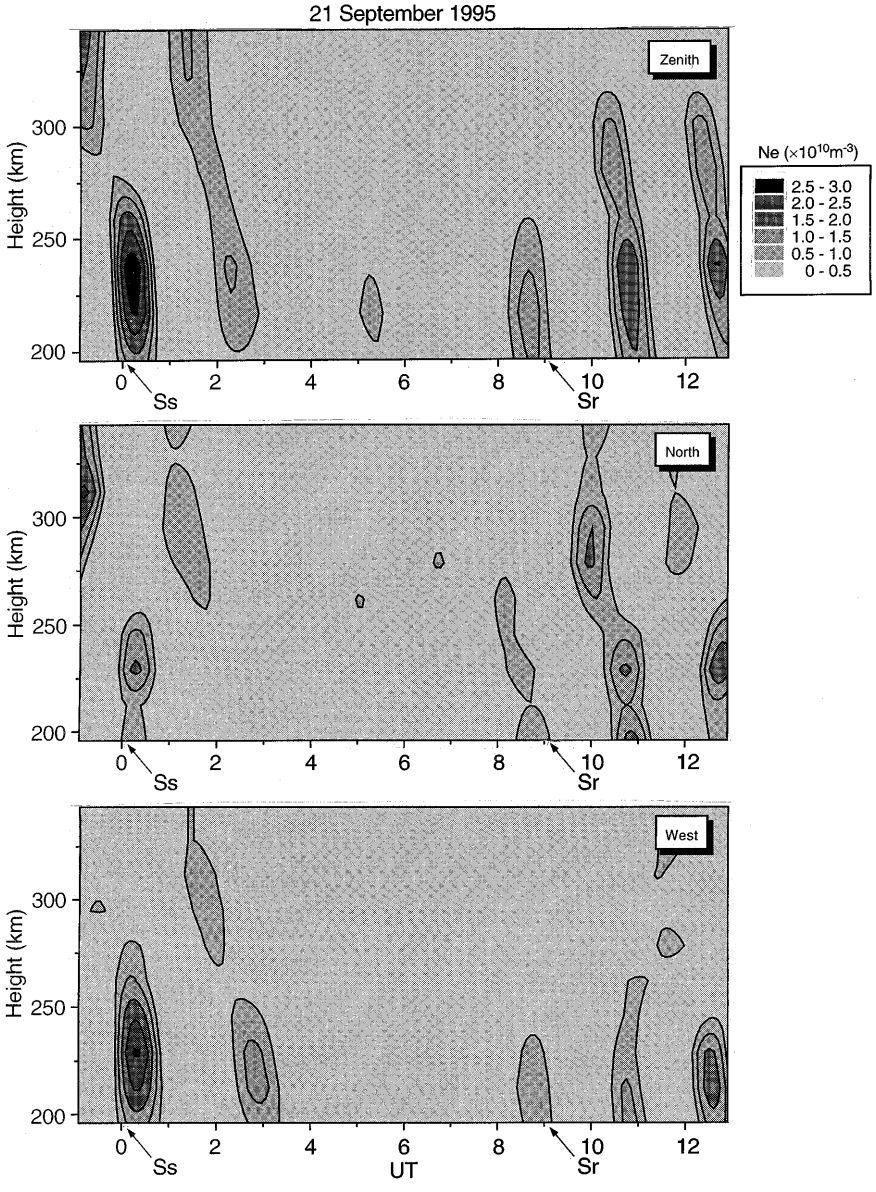

Fig. 4. Intensity of the disturbance in the filtered spectral band 90 min–130 min for the three observing positions and across *F*-region altitudes indicates intensification of the disturbances at altitudes < 300 km at the times of sunset and sunrise terminator passage

4 Discussion

The results of our investigations demonstrate that TIDs are generated by the moving solar terminator in the ionosphere. As seen in Fig. 3, the effect is observed best at sunrise, while at sunset it is rare. The measured velocity and direction of the propagation strongly

Table 1. Cross-correlation coefficient for positions Z, W, and N near the time of ST passage

h, km	W-Z	N-Z
196	0.80	0.60
217	0.83	0.75
238	0.95	0.91
259	0.90	0.87
280	0.84	0.63
301	0.62	0.45
322	0.40	0.38

Table 3. TID phase velocity and direction of propagation of the strongest (2-h) component

h, km	V_{ph}, m/s,	γ, deg	ϕ, deg
217	550	−3	17
238	193	62	253
259	268	51	212
280	165	27	−49

Table 2. TID group velocity (V_g) and direction of motion (γ elevation angle and ϕ azimuth)

h, km	V_g, m/s	γ, deg	ϕ, deg
217	475	0	101
238	343	0	98
259	268	0	96
280	268	0	96
301	236	0	120

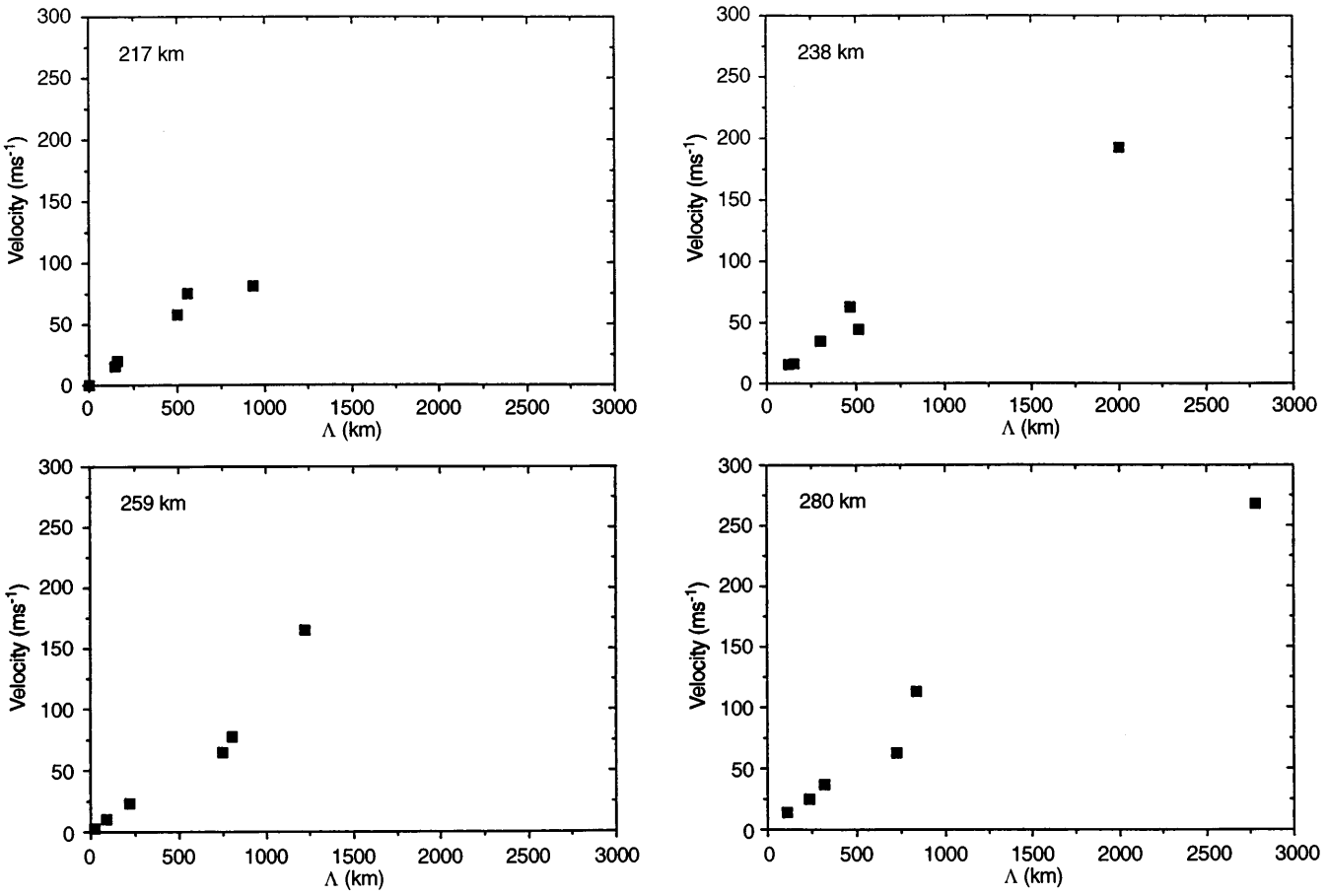

Fig. 5. V_{ph} versus Λ has been derived for the most powerful spectral components of the electron density variations for different heights. These follow the dispersion law for ionospheric wavelike processes and is evident that for longer wavelengths, the wave moves faster

indicate that the observed TIDs are associated with the ST. First, the group velocity, V_g, is close to the terminator velocity at ionospheric heights ($V_t \approx 360$ m s^{-1}). Second, propagation is directed to the west (i.e., perpendicular to the terminator). Our results indicate that the ST generates low frequency disturbances of large spatial scale. Figure 5 shows that TIDs with spatial wavelengths from hundreds to a thousand kilometers are detected most frequently. This implies that the observed TIDs are connected with internal waves belonging to the gravity part of AGW. The observations support theoretical predictions of the expected spatial scale of ST-generated TIDs, in keeping with the model of ST influence on the ionosphere described in Somsikov (1983).

It is known (Williams, 1996) that under atmospheric conditions AGW phase velocity and group velocity are perpendicular to each other. The angle between V_g and V_{ph} obtained in these experiments may be derived through a comparison of Table 2 and Table 3, whose results are given in Table 4. It can be seen that over the height range 217–259 km, the angle between V_g and V_{ph} is close to 90°. This fact indicates that the observed disturbances are of AGW origin.

Table 4. Angle between TID group and phase velocities

h, km	217	238	259	280
$\Delta\phi$, deg	84	115	105	137

An interesting result concerns the observation of horizontal motion for the TIDs (Table 2). In accordance with the accepted theory, only a wave which has a frequency close to the Brunt-Väisälä frequency is able to propagate horizontally in the atmosphere. Following Hargreaves (1979), the angle of elevation for AGW propagation can be derived as

$$\gamma = \text{atan}(\omega_B^2/\omega^2 - 1)^{1/2} \quad (2)$$

where ω is the frequency of the AGW, ω_B is the Brunt-Väisälä frequency. Consequently, if $\omega \ll \omega_B$ (which is the case) then $\gamma \approx 90°$ and the wave under consideration should propagate vertically. This contradiction probably arises from the fact that expression (2) applies to AGWs (i.e., to neutral gas variations), while charged component variations (TIDs) were measured in the experiments. The relationship between TIDs and AGWs is complicated by the necessity of taking into account the influence of the Earth's magnetic field on the motion of electron density structure in the ionosphere.

AGW parameters are closely related to the characteristics of the atmosphere. For instance, the velocity of sound in the ionosphere can be found from the ratio of phase to group velocity observed in such experiments. A new method for upper atmosphere/ionosphere diagnos-

tics using wavelike disturbances generated by the moving solar terminator is suggested, based on the interpretation of such results.

5 Conclusions

The generation of ionospheric disturbances by the moving solar terminator (ST) has been confirmed with the aid of the three-position incoherent scatter radar experiments and the use of special data-processing algorithms. It was shown that the strongest components of TIDs associated with the ST have temporal periods of about 2 h. The TIDs were shown to move horizontally, perpendicular to the terminator, and the occurrence of dominant horizontal motion seems to contradict the accepted theory of AGW/TID propagation, indicating a need for additional investigations, both theoretical and experimental. The use of ST-generated disturbances as probe signals is suggested as a new technique for atmospheric diagnostics.

Acknowledgements. The authors wish to thank the colleagues of the Millstone Hill Observatory who have taken part in these experiments. Millstone Hill radar observations are supported by the US National Science Foundation through cooperative agreement with the Massachusetts Institute of Technology.

Topical Editor D. Alcaydé thanks R. D. Hunsucker and K. Hocke for their help in evaluating this paper.

References

Beley V. S., V. G. Galushko, and Y. M. Yampolski, Traveling ionospheric disturbances diagnostic using HF signal trajectory parameter variations, *Radio Sci.* **30**(6), 1735–1752, 1995.

Bezrodny Y. G., Y. M. Yampolski, On the origin of the spatial phase deference of the VLF at sunrise and sunset period, *Izvestia VUZ-Radiofizika (Soviet Radiophysics and Quantum electronics)*, **19**(9) , 1270–1274, 1976.

Crowley, G., *Dynamics of the Earth's thermosphere; a review*, *Rev. Geophys.*, **29,** 1143–1165, 1991.

Francis S. H., Global propagation of atmospheric gravity wave; a review, *J. Atmos. Terr. Phys.*, **37,** 1011–1054, 1975.

Galushko V. G., Y. M. Yampolski, Experimental investigations of the HF signals scattered by moving solar terminator, *Izv. VUZ-Radiofiz.*, **26**(4), 499–502, 1983.

Hargreaves, J. K., *The upper atmosphere and solar-terrestrial relations. An introduction to the aerospace environment*, Van Nostrand Reinhold, 1982.

Hines, C. O., Internal atmospheric gravity waves at ionospheric heights, *Can. J. Phys.*, **38,** 1441–1481, 1960.

Hines, C. O., The upper atmosphere in motion, *Geophys. Monogr. Ser.* 18, AGU, Washington D. C., 1974.

Hines, C. O., Earlier days of gravity waves revisited, *Pure Appl. Geophys.*, **130,** 151–170, 1980.

Hocke, K., Tidal variations in the high-latitude E-region observed by EISCAT, *Ann. Geophysicae*, **14,** 201–210, 1996.

Hocke K., and K. Schlegel, A review of atmospheric gravity waves and travelling ionospheric disturbances: 1982–1995, *Ann. Geophysicae*, **14,** 917–940, 1996.

Hunsucker, R., Atmospheric gravity waves generated in high-latitude ionosphere: a review, *Rev. Geophys. Space Phys.*, **20,** 293–315, 1982.

Leitinger, R., Travelling ionospheric disturbances (TIDs) – Wissensstand und neuere Entwicklungen, *Kleinheubacher Ber.*, **35,** 1–14, Deutsche Telekom, 1992.

Mayr, H. G., I. Harris, F. Varosi, and F. A. Herrero, Thermospheric gravity waves: observation and interpretation using transfer function model (TMF), *Space Sci. Rev.*, **54,** 297–375, 1990.

Popov A. V., Y.M. Yampolski, VLF variations during sunrise period, *Izve. VUZ-Radiofiz.*, **24**(6), 1981, 794–798.

Somsikov, V. M., *Solar terminator and dynamics of the atmosphere*, Nauka, Alma-Ata, 1983.

Somsikov, V. M., and B. Ganguly, On the mechanism of formation of atmospheric inhomogeneties in the solar terminator region, *J. Atmos. Terr. Phys.*, **57,** 75–83, 1995.

Williams P. J. S., *Tides, atmospheric gravity waves and travelling disturbances in the ionosphere. Modern ionospheric science.* European Geophysical Society, Katlenburg-Lindau, FRG 1996.

Yeh, K. C., and C. H. Liu, *Theory of ionospheric waves,* Academic Press, New York-London